

SPECTROGRAPH OPTIMISATION eShel

by Christian Buil

July 2020

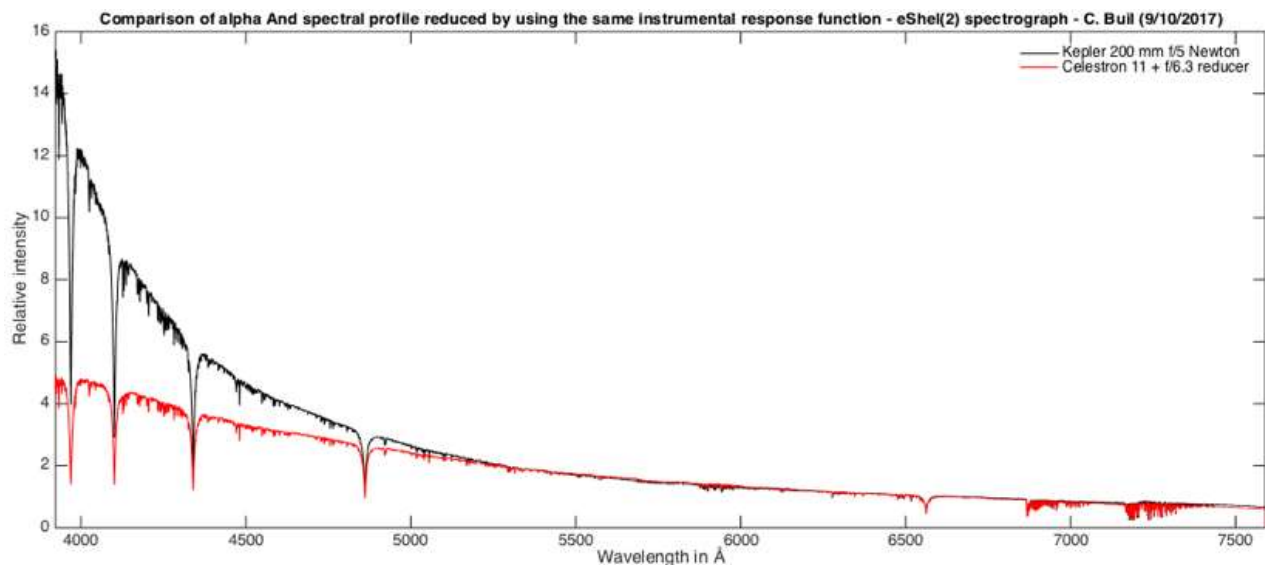


The eShel instrument is a scale-type spectrograph manufactured by [Shelyak Instruments](http://www.astrosurf.com/buil/eshel3/review.htm). Its resolution power is about $R \sim 13000$. The device is paired with the telescope through an optical fiber 50 microns in diameter. The set is complemented by a specific bet: a device that injects light from the star into the telescope's focus and is also used for guidance during poses. A description of eShel is given at this address: <http://www.astrosurf.com/buil/eshel3/review.htm>.

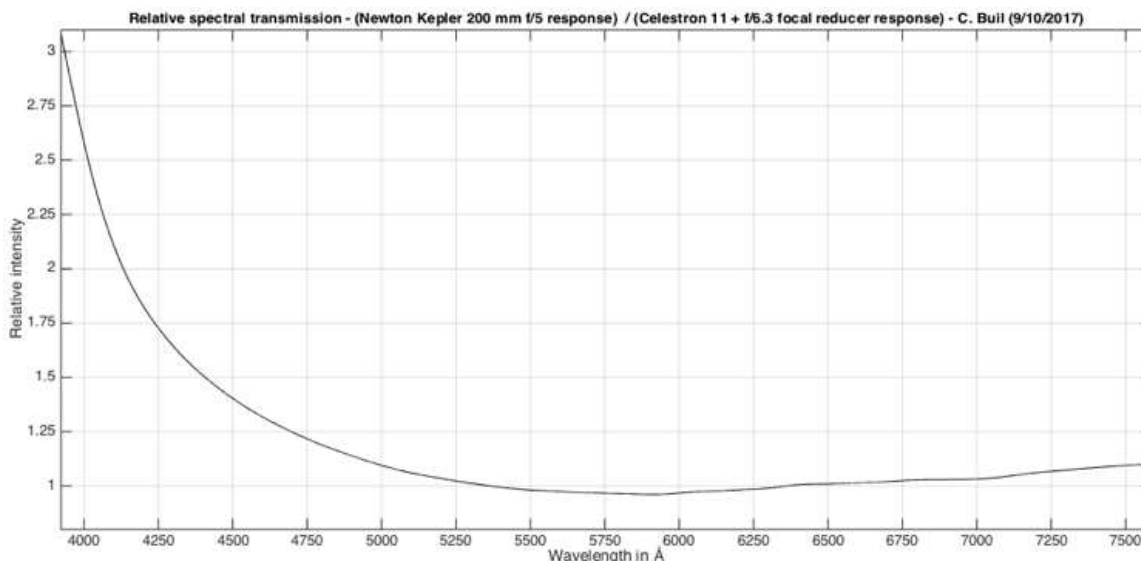
This article describes all the improvements I've made on the eShel in recent years to improve performance. Various topics are discussed, including the optical transmission of the telescope, the optics of the spectrograph, the specific characteristics of the CMOS cameras (in particular the peculiarities of the 24x36 Sony IMX455 sensor) and the processing of data (introduction of the CMED algorithm allowing optimal use of CMOS cameras in astronomy (or elsewhere).

1. The telescope

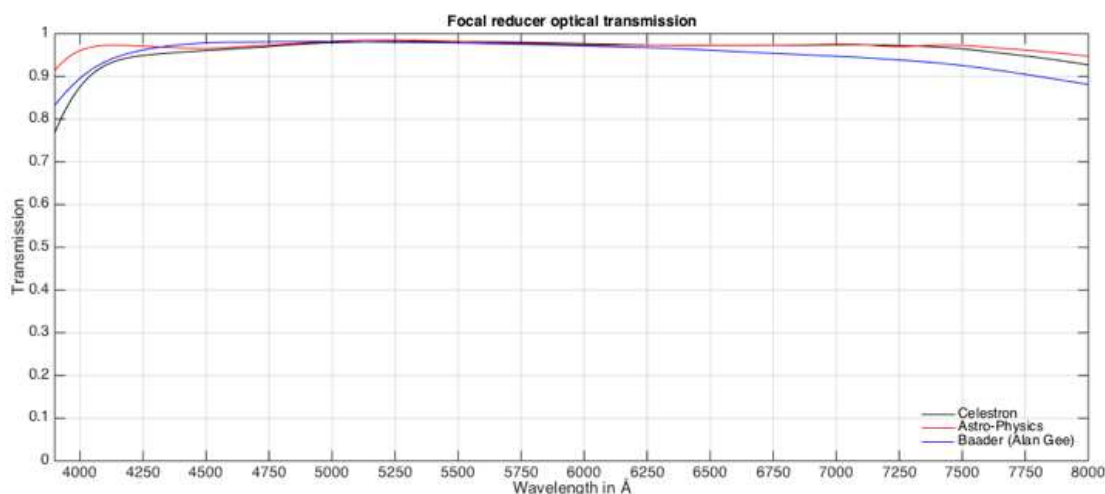
One of my goals was to improve the overall sensitivity in the blue part of the spectrum, or even the ultraviolet part, the basic eShel spectrograph showing a performance deficit at these wavelengths. But this work has to start right from the telescope. There is no point in optimizing the spectrograph if everything is ruined upstream, by a telescope that cuts the desired radiation. In this regard, there are some pretty formidable pitfalls, here is the proof:



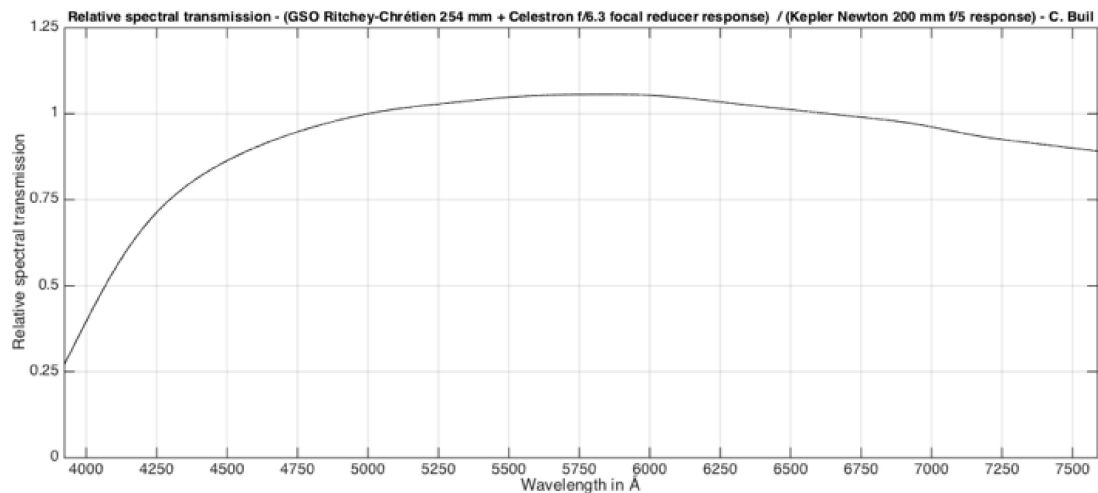
The red curve shows the spectral profile of the alpha And star, while a Schmidt-Cassegrain Celestron 11 telescope equipped with a focal length gearbox (Celestron) is used to take the aperture to f/6.3. The black curve represents the spectral profile of the same star, the same night and treated in the same way, but this time operating a Newton telescope of the Kepler brand of 200 mm diameter opened natively to f/5. The signal deficit recorded at the blue end of the spectrum using a C11 is glaring. The following curve shows the relative signal recorded between these two telescopes:



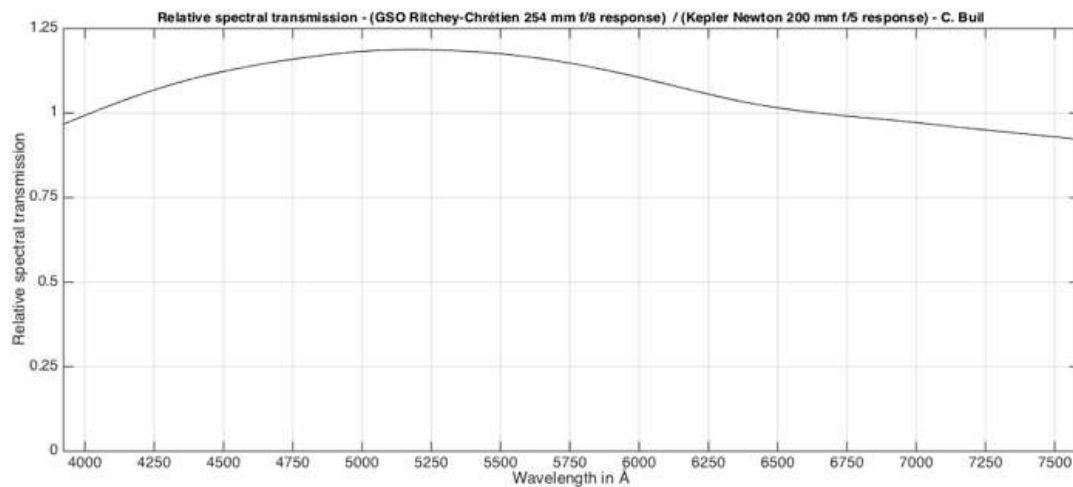
Where does this discrepancy come from? While the closing blade of a SC is opaque to ultraviolet radiation, this involves shorter wavelengths than those explored here. Similarly, modern and sophisticated anti-reflective treatments are optimized only for the visible part of the spectrum, but this cannot explain such a large gap between the two devices. Moreover, the intrinsic optical transmission of several focal length reducers was measured by the author and it appears quite neutral spectrally up to 400 nm (this is another story below 380 nm, which is important for users of the UVEX spectrograph for example):



The only explanation that really holds is the presence of chromatic aberration that affects any dioptral system (composed of lenses). One can think of the spherophoticism of Schmidt-Cassegrain, but the overwhelming majority of the problem probably comes from the focal length reducer. The subsequent relocation of stars into the blue and UV thus expanded their images in the focus of the telescope, thus reducing the amount of light reaching the spectrograph. The phenomenon increases as one dives into the deep blue. The same phenomenon can be found if the C11 is replaced by a Richey-Christian GSO (RC) telescope, which is potentially excellent (no closing blade), but deteriorated by the addition of a dioptric focal length reducer:



Again, the performance degradation in the blue of the RC equipped with a gearbox is very strong (a factor 4 compared to the Newton, whose optical formula contains only mirrors). Here's the same report when removing the focal length reducer from the RC suit:



The discrepancy is much smaller (it is suspected that the RC mirrors are covered with a dielectric treatment that increases performance in the middle of the visible spectrum but degrades the extreme wavelengths, whereas the Newton Kepler appears to have an aluminum covered with a simple silica protection monolayer, more spectrally neutral, which is ideal in fact).

One conclusion is clear: the first thing to do when trying to observe a broad spectral field is to prohibit the use of a focal length reducer (the conventional dioptric models offered in trade). This concerns eShel, but also many other equipment (Alpy, LISA, UVEX, ...).

It is also worth noting that the use of optical fibers is optimal with well-opened telescopes between f/4 and f/6. This optimizes overall performance (reducing the i.e. "Focal Ratio Degradation") and reduces modal noise (the spectral continuum is smoother and more stable over time). The acceptable high limit is f/8, which is the opening ratio of most Richey-Christian telescopes available on the amateur market, and very popular today. If you operate an F/8 RC, use it at this aperture and especially not with a focal length reducer, you understand why by reading the above. For my part, I have equipped myself with Newton telescopes (200 mm f/5 and 250 mm f/4.5) to make the best use of fiber optic spectrographs — but with the major disadvantage of excessive footprint if one aims for a larger diameter.

2. The optics of the spectrograph

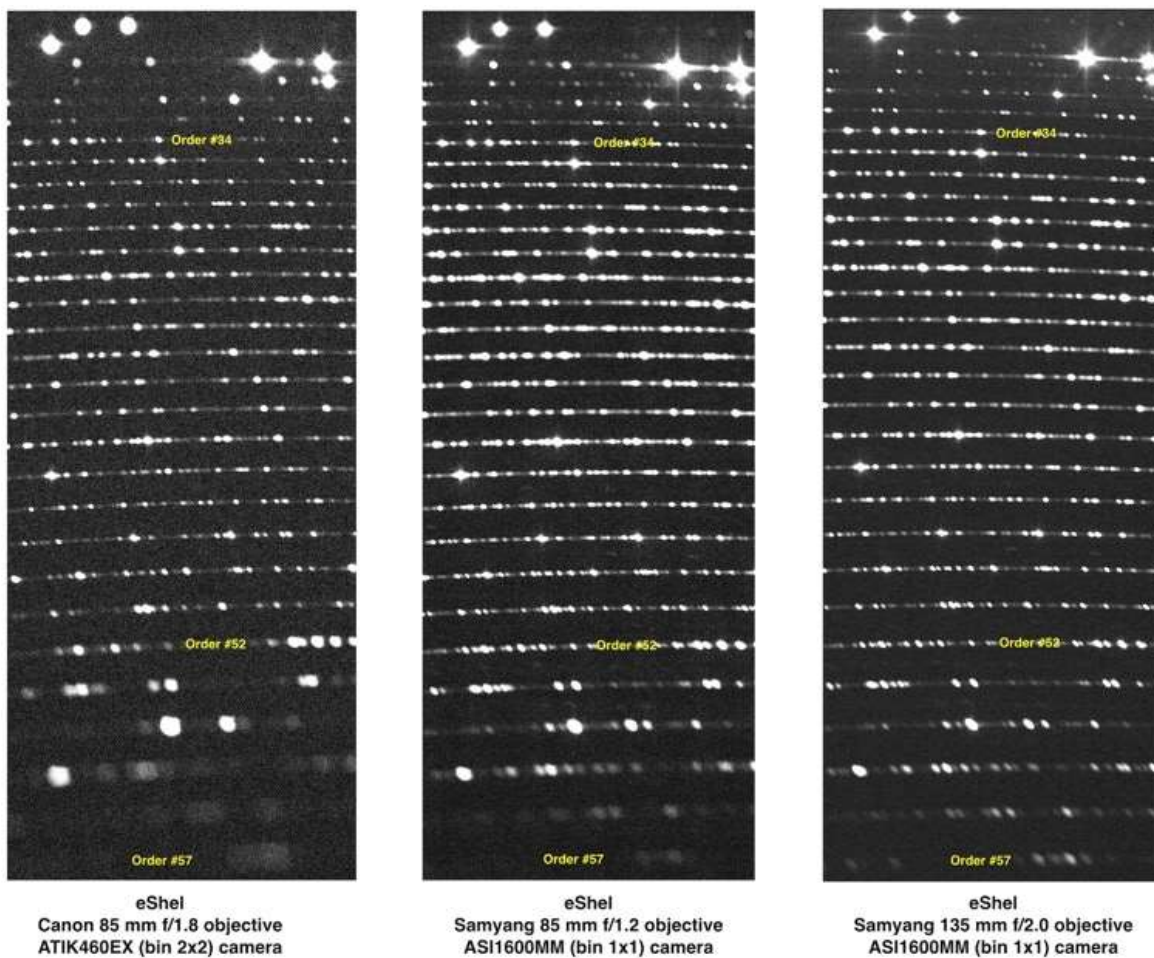
The image quality delivered by the eShel spectrograph is rapidly degraded below the 425 nm wavelength. It is still the chromatic aberration that makes these works. The blurring generated makes it difficult to operate at shorter wavelengths. Remember that eShel has two elements that have optical power and are therefore capable of generating chromaticism: the achromatic doublet constituting the collimator and the camera lens, an 85 mm Canon photographic optics of focal length open to f/2.8.



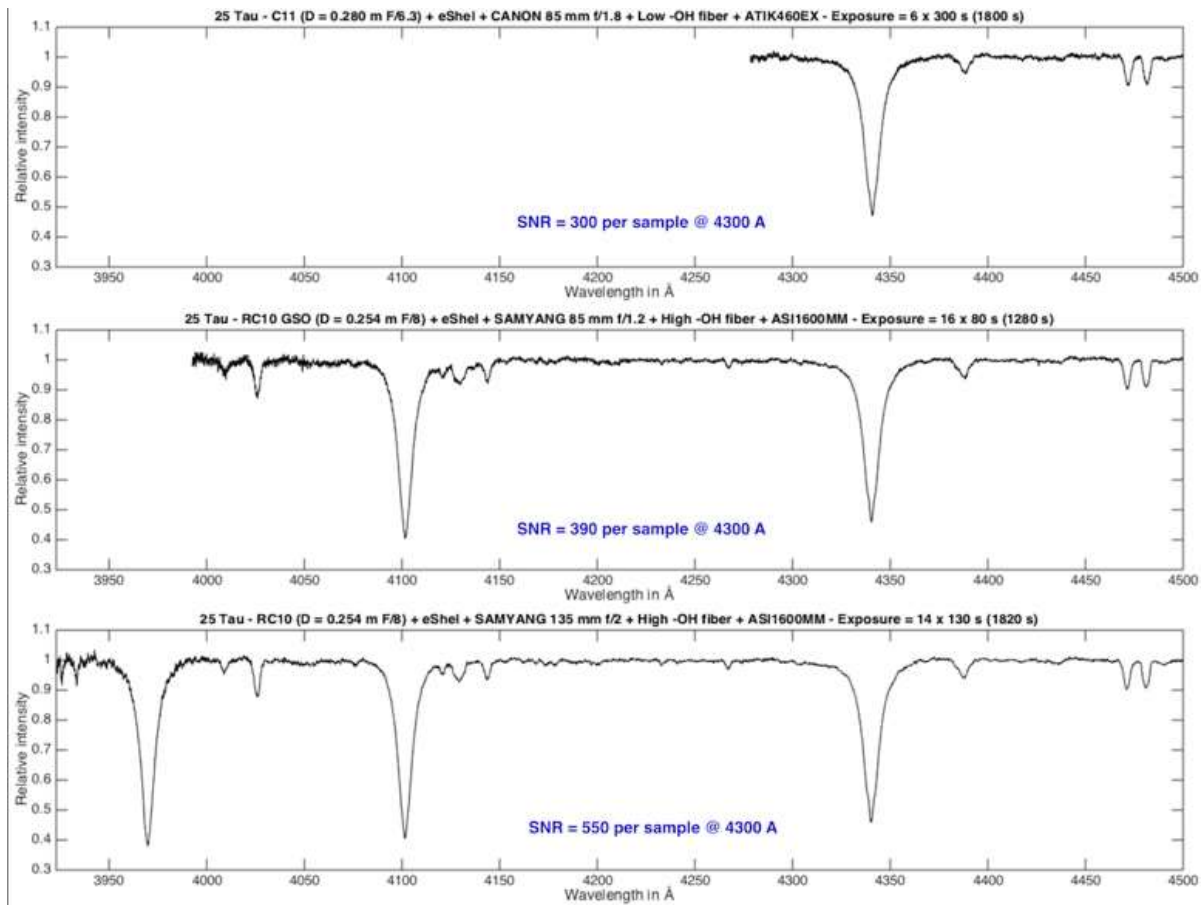
The first action was to work with Shelyak to achieve a better corrected doublet collimator, then look for better quality photographic lenses than the basic 85 mm f/2.8, and finally, find out if it was not possible to compensate the chromaticism of the collimator with that of the lens in order to form an apoeatic chrome set without turning everything upside down in the spectrograph.

This research went through the photographic optics Samyang, very effective on paper and inexpensive because very stripped down. In fact, for the traditional photographer and astrophotographer, the image dive delivered by these lenses, often very bright, is really good, and the construction excellent for the price (I've seen brand lenses much more off-center and shockingly bad in my career!). Here, for example, is the eShel spectrograph equipped with the spectacular Samyang 85 mm /1.2 lens and an ASI1600MM camera (CMOS sensor). I also tested the Samyang 135 mm f/2 in the same situation.

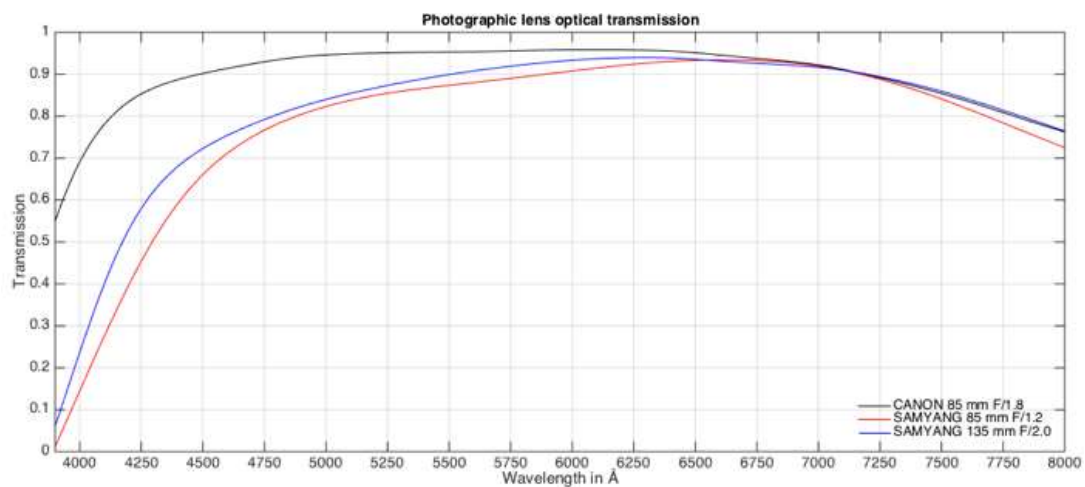
It soon became apparent that all these replacement optics were of a higher quality than the Canon 85 mm f/2.8 lens, at least in the context of use with eShel. The following document shows an excerpt from an image of the Thorium-Argon spectrum following the chosen camera lens (capture is done with an Aik460EX camera with the basic lens and with an ASI1600MM camera for testing with Samyang lenses, the largest CMOS sensor I had access to at the time of these tests).



With the Canon 85 mm f/2.8 chromaticism is strong in the lower part of the image (widening of the rays), an area corresponding to the blue part of the spectrum. The Samyang lens of 135 mm f/2 has raised great hope by extending the exploitable spectral domain of 4 orders of diffraction in the blue, which is a very strong grain. Of course, this long focal length involves the use of a larger detector to capture the entire image of the spectrum. But this is good with the arrival of quality CMOS sensor for a relatively modest price (compared to CCD), like the Panasonic sensor that equips the ASI1600MM camera. A very nice technical conjunction! Here is the same comparison, but in the form of a spectral profile, that of star 28 Tau (the continuum is adjusted for better legibility):

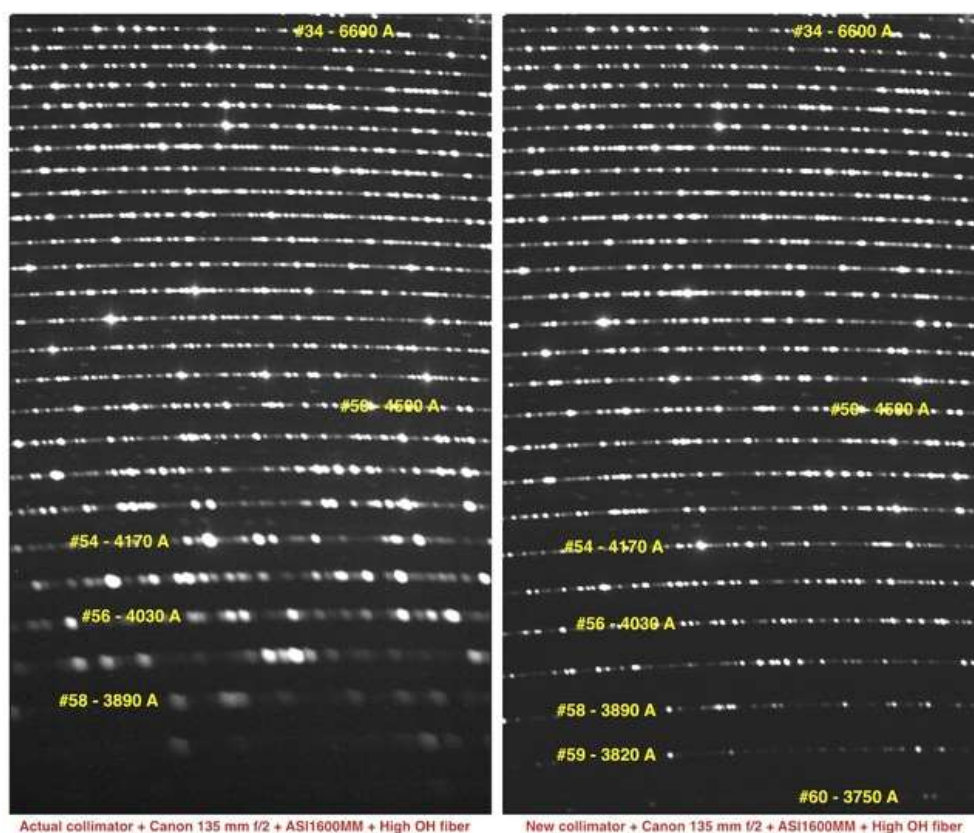


Unfortunately, a flow deficit was quickly spotted in the blue with Samyang goals. The measurement of the optical transmission of all these objectives confirms this point (measured by the author with a LISA spectrograph):

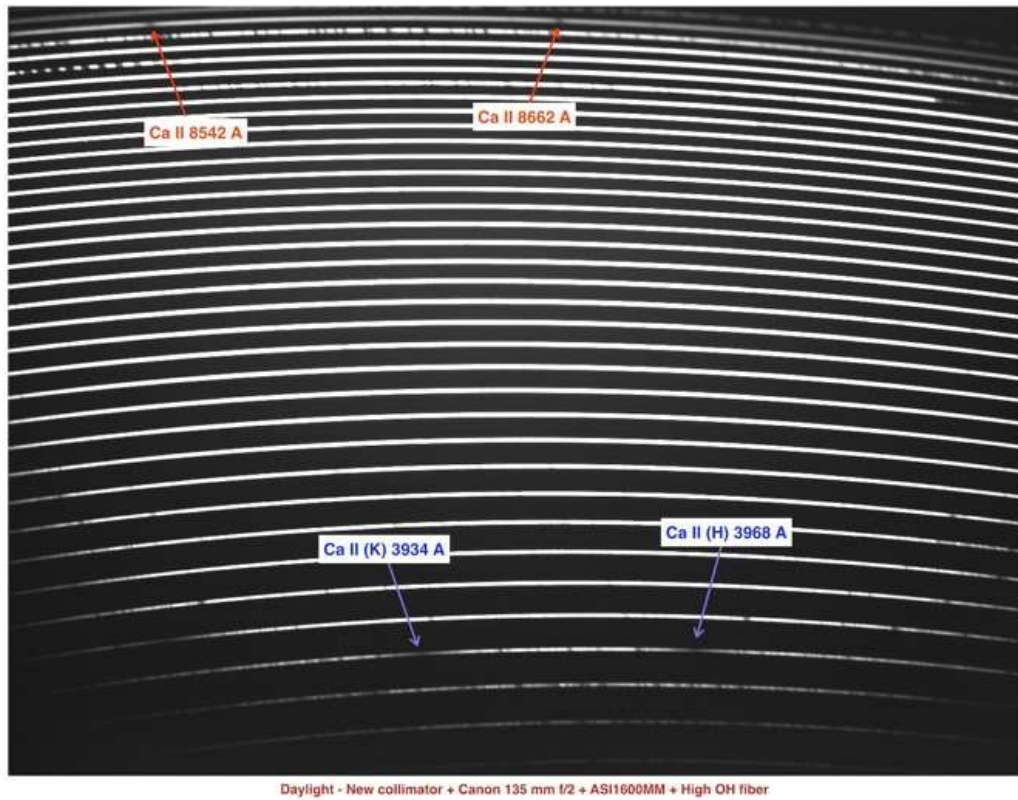


The optical transmission of the Samyang lenses tested collapses below 400 nm (both the 85 mm and the 135 mm). This is not going to bother the photographer, and it is even rather an advantage for him because the lens cuts by itself the harmful ultraviolet radiation because of the poor optical correction of the lenses in these wavelengths. This is another case for spectrography, where the thing is totally prohibitive (because no signal is to be measured in the end). The technical explanation is not known officially, but I suspect that Samyang optics feature plastic lenses to lower the cost. If this is the case, this does not mean that these optics are bad qualities, on the contrary, because we know how to make plastic lenses as effective as glass lenses for the conduct of light rays. No worries with that.

Unfortunately optical transmission suffers, and seriously for us. But the track of a long focal length to equip eShel is correct, and finally, the right pick was the Canon 135 mm f/2 L Series lens, more conventional and more expensive, but very good for our application. In addition, the coupling with the new optimization of the collimator has allowed to achieve a form of apochromatism allowing to observe the spectrum with the theoretical near spectral resolution up to about 3750 Å, which is remarkable. The following images show the very good pairing found between the new collimator (available from Shelyak) and the Canon 135 mm f/2:



Below, the entire image of the Spectrum Scale of the Sun, in the optimized optical version of eShel (note the wide spectral coverage from the Infrared Ca II rays to the ultraviolet Ca II rays and beyond):



Conclusion of this part: to optimize the operation of eShel, this provide the new collimator, buy a Canon lens 135 mm f/2 or equivalent, use a large-format sensor to capture the entire spectrum. All this has a financial cost unfortunately, but it is also the price of a superior performance.

3. Fibre optics

The concentration of OH in a fiber determines the level of attenuation of the optical flow over its length. For minimal reduction in the visible and ultraviolet, a so-called "high-OH" fiber must be selected. Shelyak can provide this type of fiber, but you can also buy it easily at [ThorLabs](https://www.thorlabs.com) with the features that suit you best (length, type of sheath, ...). I am currently using a 50 micron FG050UGA multimode ThorLabs fiber with a 15-metre-long metal sheathing (the connector is of the FC/PC type). I use the equivalent in 200 microns to drive the calibration source, again over a length of 15 meters.



Scramblers shake the science fiber slowly and continuously over a wide range. I use the large amplitude oscillatory motion of domestic fans on which a portion of the length of the fiber is attached. This rudimentary scrambler system blurs the modal structure of the fiber and significantly decreases the artifacts in the spectra, induced by the propagated modes, which can be likened to modal noise. Few eShel users use this type of device, yet... On this page: http://www.astrosurf.com/buil/modal_noise/ an article on this issue.

4. Temperature regulation

A change in the operating temperature of the spectrograph results in a calibration error of about 3 km/s per degree, or about 0.055 angstroms in the center of the visible spectrum due to the variation in the air refraction index. This effect is discrete, but it can be detected with an eShel spectrograph and therefore proved troublesome for high-precision work. Most importantly, temperature regulation reduces the risk of thermoelastic deformation of the spectrograph, a major cause of calibration error in the end. The view on the right shows the eShel spectrograph permanently housed in a wine cellar where a temperature is maintained close to 10°C, with a fairly satisfactory stability in the state of $\pm 1^\circ\text{C}$. The instrument is here team of the lens of 135 mm f/2 and an ASI6200MM camera. Another advantage offered by the wine cellar is the ability to descend to a fairly low operating temperature of the sensor, here -15°C in this case with the indicated camera. This low temperature contributes to the detection of weak objects by lowering thermal noise.



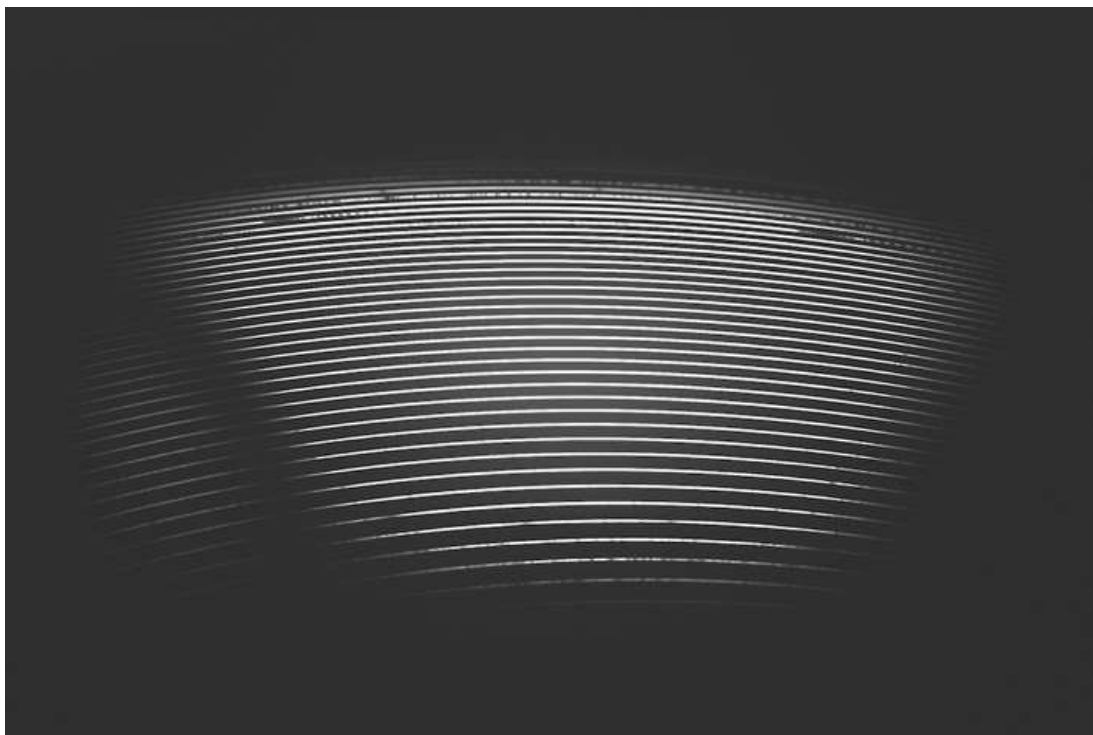
5. The detector

In spectrography, and especially in scale spectrography, the value of reading noise is quite decisive: the weaker it is the better. The noise of the sky background is generally very low in spectrography, if not zero, it is the reading noise (the noise of the thermal signal) that dominates. This noise is called RON, for Read Output Noise. In today's CMOS sensors, it is between 1 and 2 electrons, while it is 4 to 6 electrons in the CCD cameras which its equipped amateurs. This exceptional low value in CMOS is a potential asset in spectrography (less in deep sky imaging, for example, where photon noise from the sky background is generally dominant). Unfortunately, other sources of noise are added (these are pseudo-noises), but it is possible to reduce them well by an appropriate digital processing, described in the next section.

I use here a very recent camera at the time of writing this article, ASI61200MM([ZWO](#)) equipped with the CMOS Sony IMX455 detector, of imposing size, and of which here are the main characteristics measured during this work of optimization of eShel:

Nombre de pixels	9976 x 6380
Taille des pixels	3,76 microns
Gain électronique réciproque (pour gain caméra de 100)	0,26 e-/ADU
Bruit de lecture (gain=100, T=-15°C)	1,6 e-
Signal d'offset (gain=100, offset=20)	200 ADU
Capacité de charge sur 16 bits	17 000 e-
Dynamique vraie	13,5 bits
Taux de signal d'obscurité (T=-15°C)	0,00049 e-/s
Rendement quantique système à 550 nm	73 %

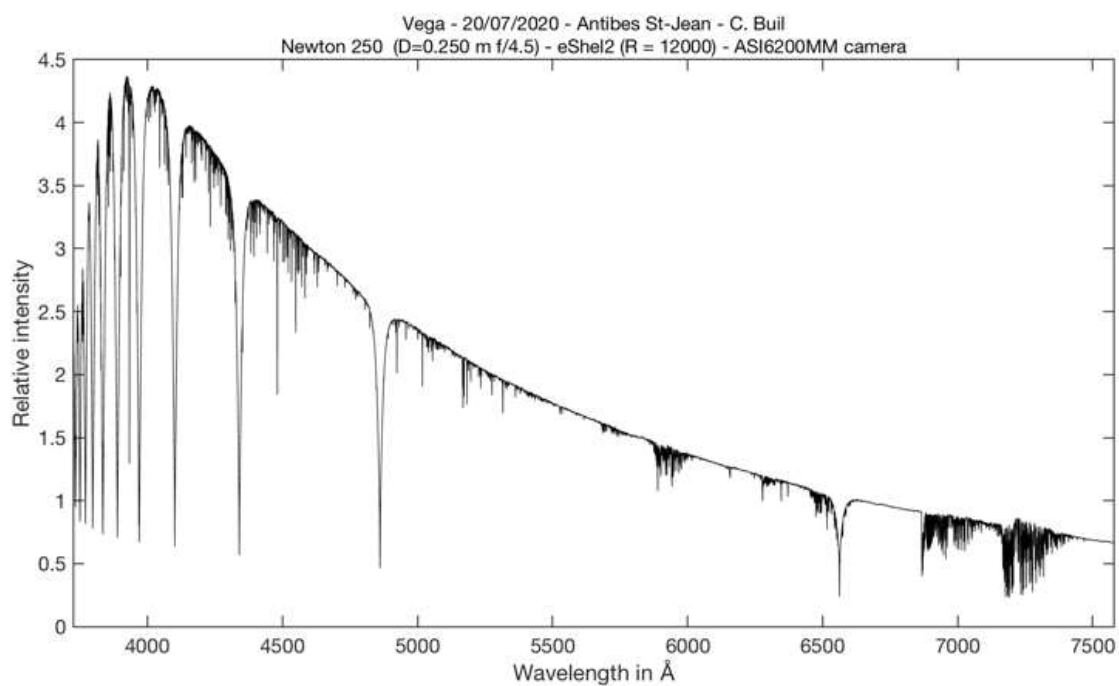
What the table does not indicate, are two strong break points compared to the older generations of CMOS sensor: the total absence of electroluminescence (even after a very long installation time, an hour for example) and the scanning on 16 bits, or 65536 levels or ADU (while for most previous models, the scanning is done on 12 bits, sometimes only 14 bits). We are entering the adulthood of the CMOS. Another highlight is the large size of the 24x36 sensor. This is generous and allows to capture the entire spectrum scale delivered by the eShel spectrograph with a good margin, including with a 135 mm focal length lens, as shown in the following image of the full-format solar spectrum:

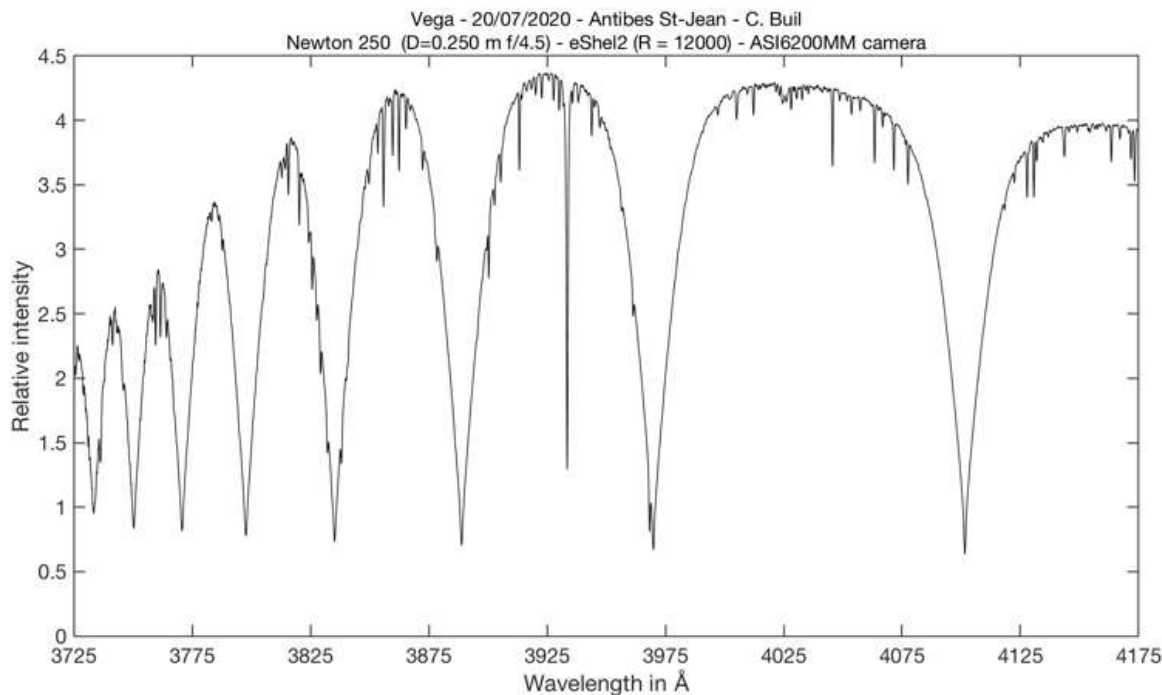


Of course, during actual acquisitions, only the just useful portion is backed up on the disk (windowing reduces the size of the images in this case by a factor of two, and also the time spent on calculations). Warning, in CMOS there is a golden rule: you must ALWAYS acquire spectral data in binning 1x1 in order to give this the means to reduce the noise later, even if the files still look big, here 117 MB after the windowing. Here is the image the look of the image "cropped":

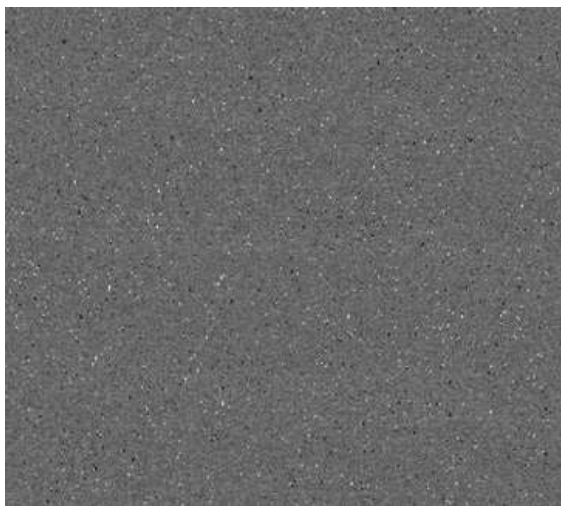


Thanks to this equipment and the applied processing, I can acquire spectra up to the wavelength of 3725 Å (order 60), which is a first for the eShel spectrograph. For example, below is the spectrum of the bright Vega star, which classically serves as a reference object;



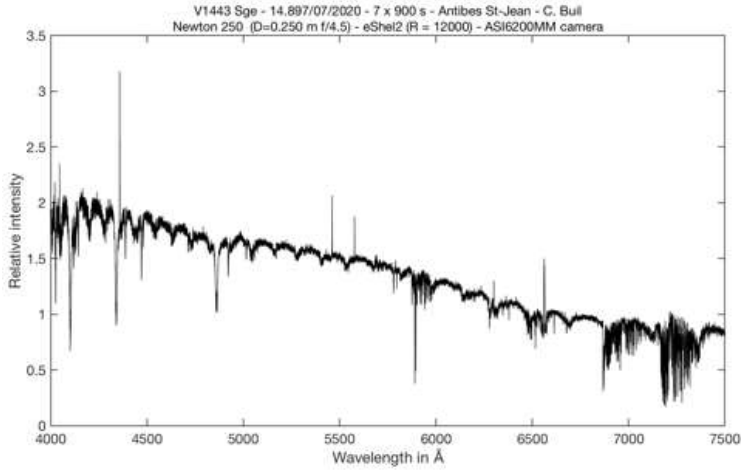


Unfortunately, as in all CMOS sensors tested so far, the IMX455 has a typical defect in the form of a load generation rate that varies abruptly and randomly over time, producing a signal called random telegraph signal (RTS, Random Telegraph Signal). As a result, the histogram of the reading noise moves away from the ideal Gaussian shape (characteristic of CCD sensors). Here is a very high-contrast image of the offset signal of the IMX455 that shows the RTS (scattered and isolated pixels whose level rises or drops significantly compared to the average level):



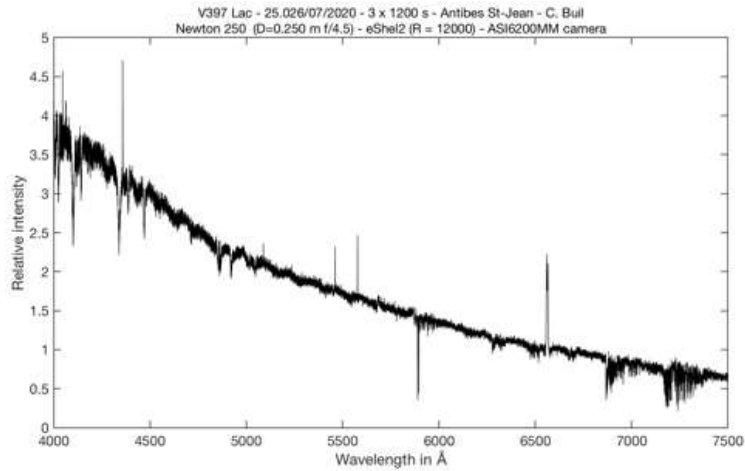
This noise structure evolves more or less quickly over time, making the defect impossible to calibrate (it's a $1/f$ noise). Note that the RTS is not unique to IMX455, it is found in all CMOS, and in particular the popular IMX183. Note again that the RMS noise of 1.6 electron shown in the performance table above takes into account the telegraph noise, which means that it is quite discreet, fortunately. But we will still try to eliminate it through a process described in the next section.

A question that comes up very often when using a CMOS sensor is the setting of the "gain" and "offset" parameters. These settings are possible in CMOS, not CCD, which confuses users of these latter sensors. The IMX455 case is special because from the gain of 100 (in ZWO terminology), the reading noise is almost constant, between 1.5 and 1.6 electron. For common uses, it is therefore in interest to work with the gain of 100, case besides the lowest noise, it also offers maximum dynamic.



But it's not that simple. I have noticed a subtle problem when you settle on the gain of 100 and work with very weak signals (some ADU): the correction of the blaze function is degraded compared to what is when the signal is stronger. It seems a may have been close to that this sensor, and suspects of other CMOS, suffers from a non-linearity response defect to very low signal signals (some electrons to dozens of charge electrons). The spectral profile opposite shows the phenomenon on a magnitude 9 star, with typical waves indicating that diffraction orders are not well connected to each other, while the result is much better for a star of magnitude 8 or brighter for an identical unit pose time.

The spectrum on the right is that of a star of magnitude 9.7 achieved this time with a gain of 200. The restitution of the continuum is much more satisfactory. Conclusion: Even if it loses momentum, I recommend adopting a gain of more than 100 for your low flow observations. For the part, I adopted a gain of 200 and an offset set to the value 60 (which in the case of the camera ASI6200MM produces an offset whose average level is 600 that avoids truncating noise in very weak signals). Note that the authors of the ASCOM driver of the ASI6200MM camera do not currently allow a gain greater than 100, which corresponds to a degradation of an element of the performance of the camera, admittedly little known, but real, the problem of non-linearity.



I use here the native driver of the Prism software, which does not have this limit in gain. The following table compares asi6200MM camera settings for 100 and 200 earnings:

Gain électronique (pour gain caméra de 100)	0,26 e-/ADU
Bruit de lecture (gain=100, T _e =-15°C)	1,6 e-
Signal d'offset (gain=100, offset=20)	200 ADU
Gain électronique (pour gain caméra de 200)	0,080 e-/ADU
Bruit de lecture (gain=200, offset=60)	1,5 e-
Signal d'offset (gain=200, offset=60)	600 ADU

The quantum "system" performance of the ASI6200MM camera was evaluated through an intensive inter-camera comparison campaign. At the minimum, the relative values between cameras shown in the following table are correct. By QE "system," I mean a performance that includes the optical transmission of the window that closes the camera and the fine window that covers the sensitive surface of the detector. On the face of it, the manufacturers give the quantum performance of the naked photosensitive chip, which may explain values measured here slightly lower than those they generally provide.

λ	KAF-3200 Kodak CCD (QSI532)	ICX694AGL Sony CCD (ATIK460EX)	MN34230PL Panasonic CMOS (ASI1600MM)	IMX183 Sony CMOS (ASI183MM)	IMX455 Sony CMOS (ASI6200MM)
3800 Å	51%	39%	35%	44%	37%
4000 Å	59%	59%	50%	67%	63%
4500 Å	64%	68%	62%	78%	77%
5000 Å	72%	70%	64%	79%	80%
5500 Å	80%	67%	56%	71%	73%
6000 Å	82%	57%	49%	59%	59%
6500 Å	83%	49%	40%	48%	49%
7000 Å	71%	43%	31%	44%	45%
7500 Å	59%	37%	22%	35%	37%

We notice that the quantum performance measured on an ASI183MM camera and an ASI6200MM camera is remarkably similar, except in the deep blue, where the performance of the camera is slightly receding, which is a disappointment. It is likely that Sony uses a very similar manufacturing process for the IMX183 and the IMX455. Moreover, the 90% peak quantum yield sometimes displayed for the IMX455 seems very optimistic. The absolute value of the performance is more likely to be closer to that shown in the table (80%, or 82% at best if the transmission of the various windows that passes through the light to the photosensitive chip) is taken, which is already a very good performance. The simple visual examination of the light reflected by the surface of the IMX455 does not indicate a deep black detector that characterized a 90% efficiency (just to the eye and with a little experience, it is indeed possible to evaluate the EQ - for example a thin detector with a yield of 95% is almost black as coal, because only 5% of the incident light is returned to the eye, the rest being absorbed by the sensor, which is the intended purpose.)

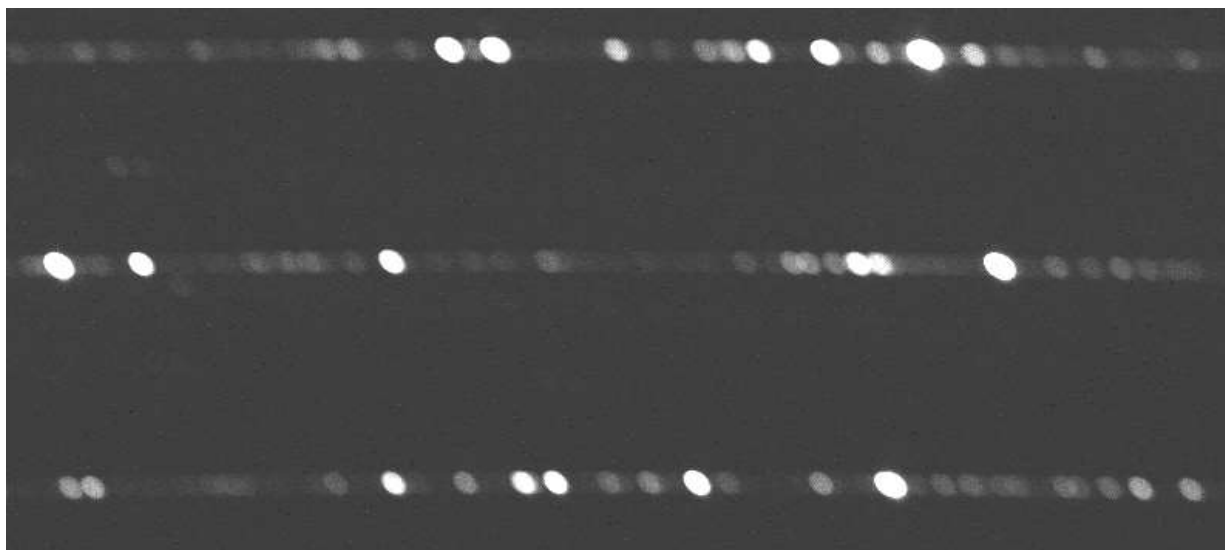
5. Data processing

The small pixel size of most CMOS sensors (3.76 microns for the IMX455) is sometimes considered detrimental to performance in low-flow detection. In reality, this small size can be used to filter VERY efficiently the RTS noise and more generally, all the noises of the detector, until reaching a level well below 1 electron RMS on the offset image. This is the idea of the CMED algorithm ("for CMOS Median"), which I developed and describe in this section (see also an application for data from the UVEX spectrograph here: http://www.astrosurf.com/buil/UVEX_soft/)

The aim of CMED is thus to enhance the small size of pixels, which means that images acquired with a CMOS sensor are often over-sampled, at a spatial frequency far greater than the optical frequency. Therefore, it is legal and easy to filter a large part of the RTS noise by applying a simple median spatial filter to the image acquired in full resolution, i.e. in binning 1x1. The median filter is a filter whose non-linearity is sometimes a problem in image processing: it can generate artifacts and photometric errors. But the way it is applied here greatly reduces this defects. These are somehow masked by the high frequency of sampling. The algorithm also includes a step to reduce the size of the image by pixel agglomeration - an operation called binning - which further blurs potential defects. Here is the whole processing done in the CMED context, the algorithm itself for steps 3 to 6:

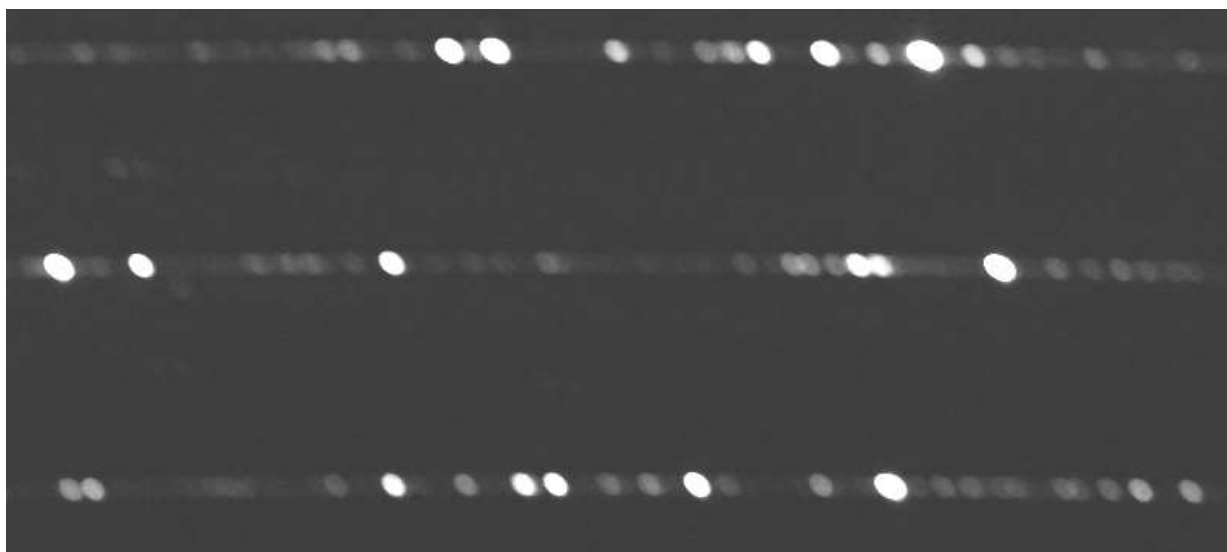
- Step 1: Always make acquisitions in 1x1 binning.
- Step 2: Make the classic pre-treatment by remaining in binning 1x1: subtraction of the offset (or bias), the signal of darkness, division by the flat-field.
- Step 3: Apply 3x3 median filtering (possibly 5x5 in very strong over-sampling situations - see below).
- Step 4: Optionally, allow yourself to perform a slight Gaussian spatial filtering. This filtering helps to eliminate the artificial effect of the median filtering of the previous step and helps to further reduce noise.
- Step 5: Binning the image of a factor that preserves the spatial resolution of the image in order to further reduce noise and to lighten the size of the images, usually a 2x2 or 3x3 binning.
- Step 6: Exploit the resulting image in a classical way (geometric corrections, optimal spectrum extraction, scientific analysis, etc.).

To illustrate in a concrete way how the algorithm works, let's take the example of a detail of the image of the Thorium-Argon taken in binning 1x1 in its raw form (it comes out of the detector):



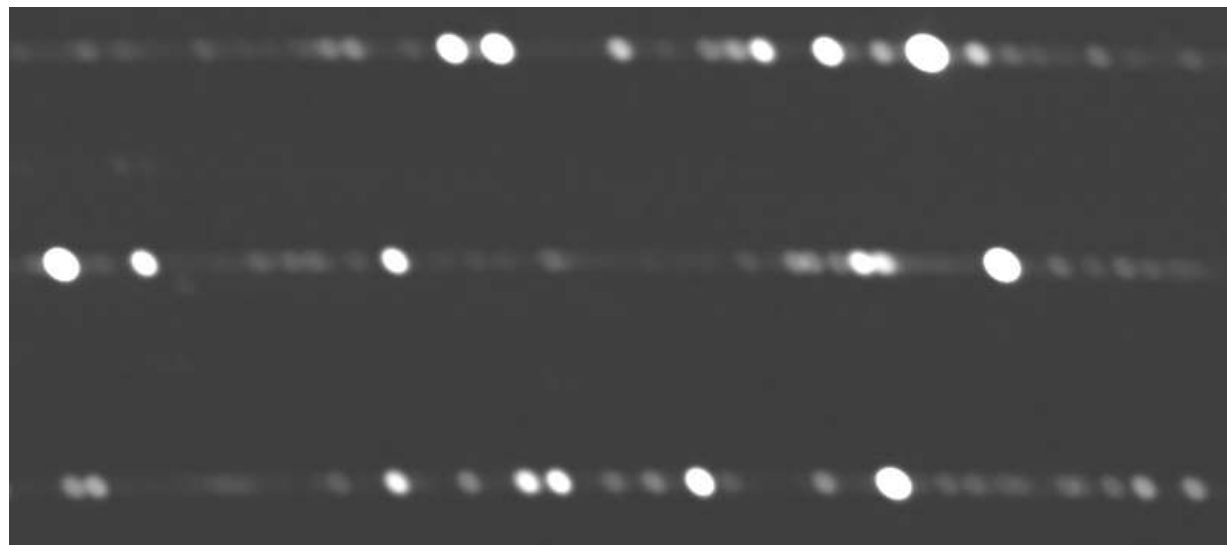
Several comments are needed. First, as equipped (new collimator and Canon 135 mm f/2 lens), eShel delivers a very clear image of the fiber of 50 microns (we can see its outline). Probably too sharp even, because the boxy character of monochromatic rays can be a cause of pseudo-noise errors. In addition, monochromatic fiber images are elongated and tilted due to optical anamorphosis and geometric distortions, normal problems in this type of spectrographs, very well corrected in the subsequent data processing. Finally, and most importantly, the images of the slot appear massively over-sampled by the small size of the pixels. Concretely, around the H α ray the spectral sample is 0.048 Å/pixel when working in 1x1 binning. The resolution power, given the diameter of the fiber is $R = 13000$, i.e. an FWHM of $6563 / 13000 = 0.505$ Å. Given the sampling factor by pixels, the half-height width of the monochromatic lines in pixels is $0.505 / 0.048 = 10.5$ pixels. This is well above Shannon's 2 pixel/FWHM limit. Oversampling is effective.

The following document shows the result after 3X3 median filtering (under ISIS you can use the MEDIAN online command to manually test the result):



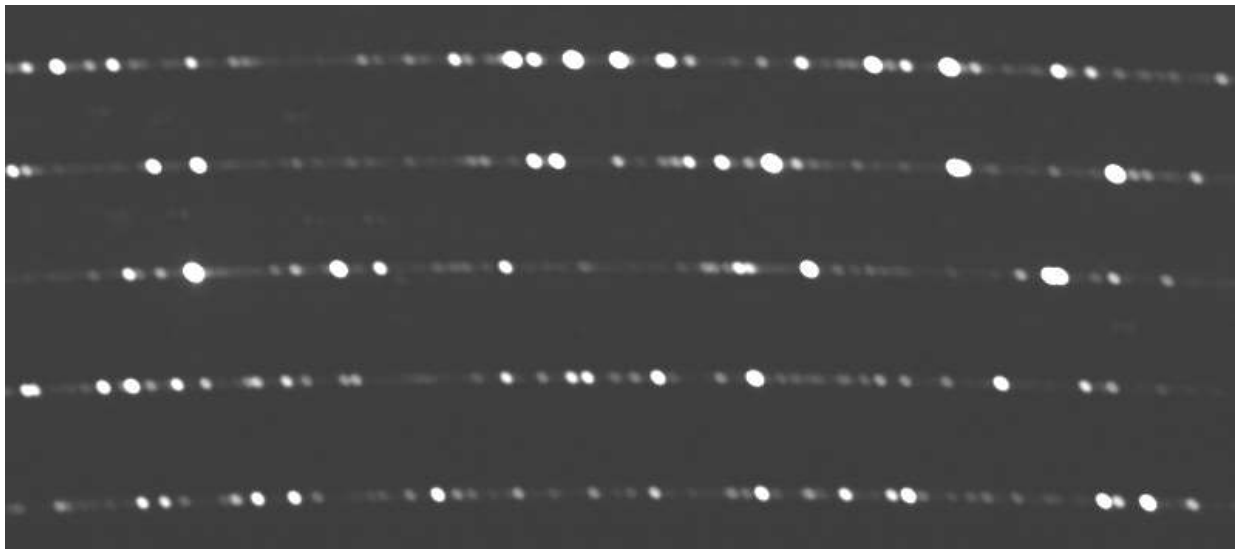
Despite the application of this filter, no spectral degradation is observed, which is fundamental here. The images of the fiber are always as well defined. Moreover, this 10-pixel/FWHM sampling would almost allow for median filtering with a 5x5-pixel core, but I wanted to keep a margin to avoid any risk of artifacts (a 5x5 core can be suitable from 13 pixels/FWHM).

In the unfolding of the algorithm, then comes optional Gaussian filtering (online command, GAUSS2):



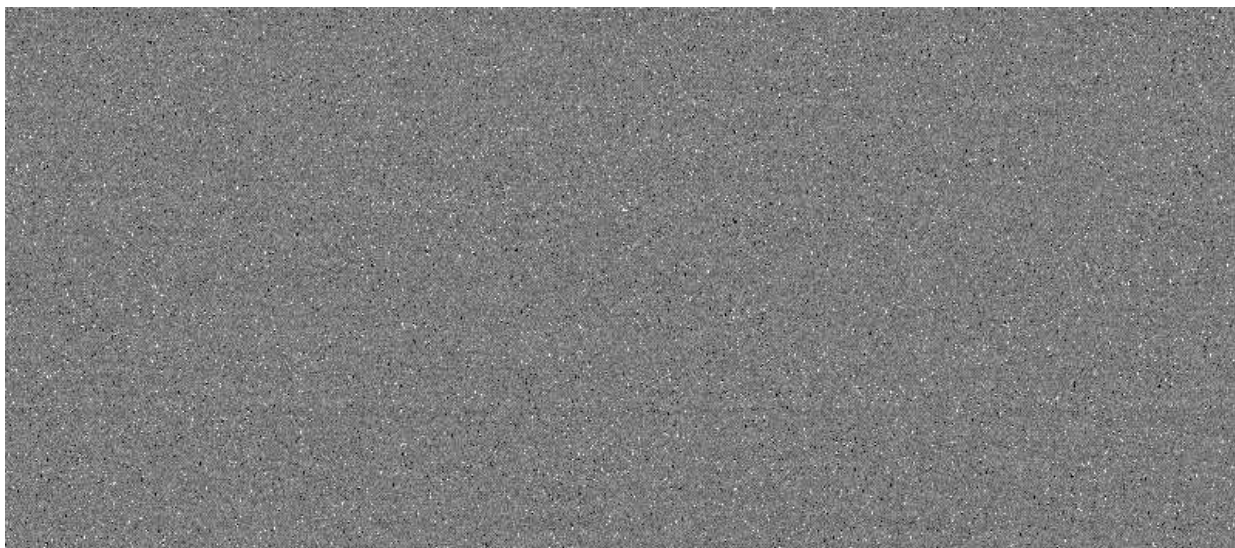
The convolution core here is 4.7 pixels of FWHM, and corresponds to the command "GAUSS2 2" under ISIS (if you do GAUSS2 4, the FWHM filter is $2 \times 4.7 = 9.4$ pixels, and so on). This time a blurring effect appears in the image, but it's intended. It breaks the boxy appearance of fiber images, while little altering the resolution power. Let's do the first-order assessment of the loss of spectral resolution. An image with a pulse of 10.5 pixels per Gaussian core of 4.7 pixels is convoluted. Considering the quadratic sum of the effects, the final FWHM is 11.5 pixels. This means that eShel's resolution power goes from R-13,000 in native, to R -12,000 after convolution. This degradation of resolution remains modest, especially since the quality of the spectrum is improved in terms of the reliability of the spectral profile thanks to the Gaussian form of the generated implusion.

Finally, the size of the image is reduced by a factor of 2 per agglomeration (binning) 2x2 pixels (BINXY command under ISIS):

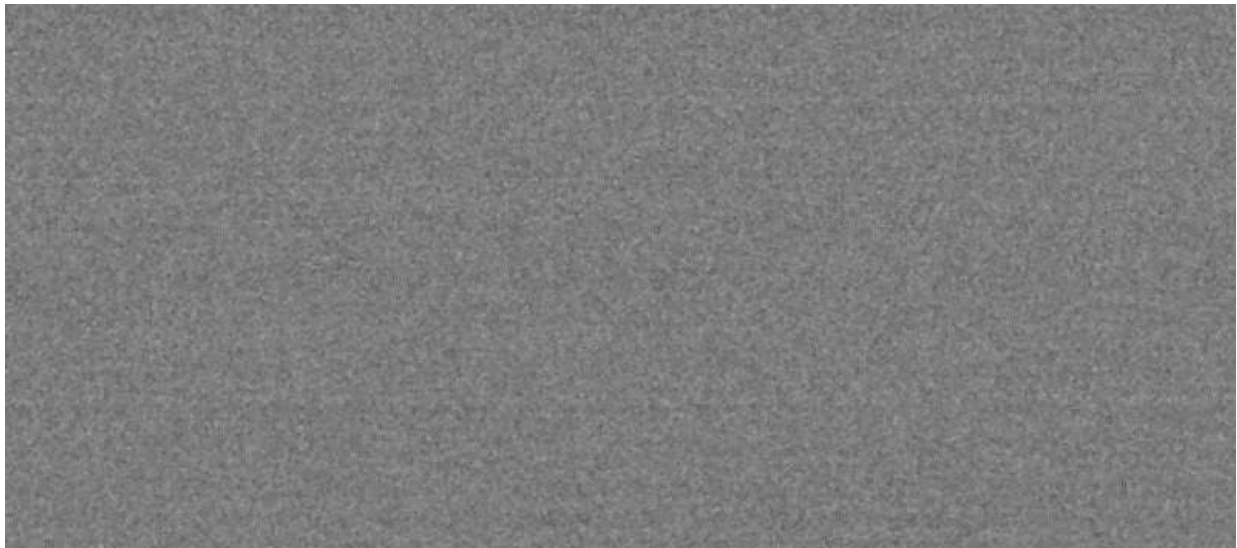


Binning may reduce noise and, above all, it lightens future treatments. It is perfectly legitimate here because once the binning is done, the sampling factor of monochromatic lines remains high, about 5.7 pixels/FWHM, which allows to treat with great serenity the spectrum in the aftermath of operations (geometric corrections without artifacts, preservation of resolution power, high accuracy of spectral calibration).

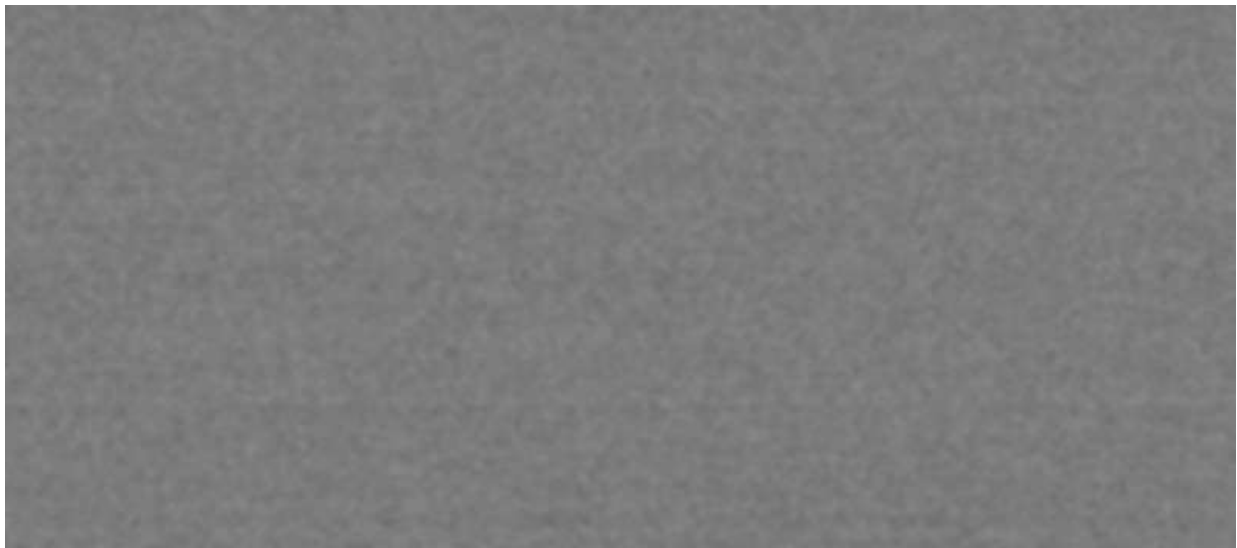
But what exactly is the benefit of all these transactions, which may appear complex at this stage? To assess it, you have to analyze the noise at each stage. Let's see what happens to the image of the offset signal to each of them, the offset signal containing the signature of the reading noise (and the RTS noise). Here is the image of raw offset in 1x1 binning and high contrast to bring out the noise:



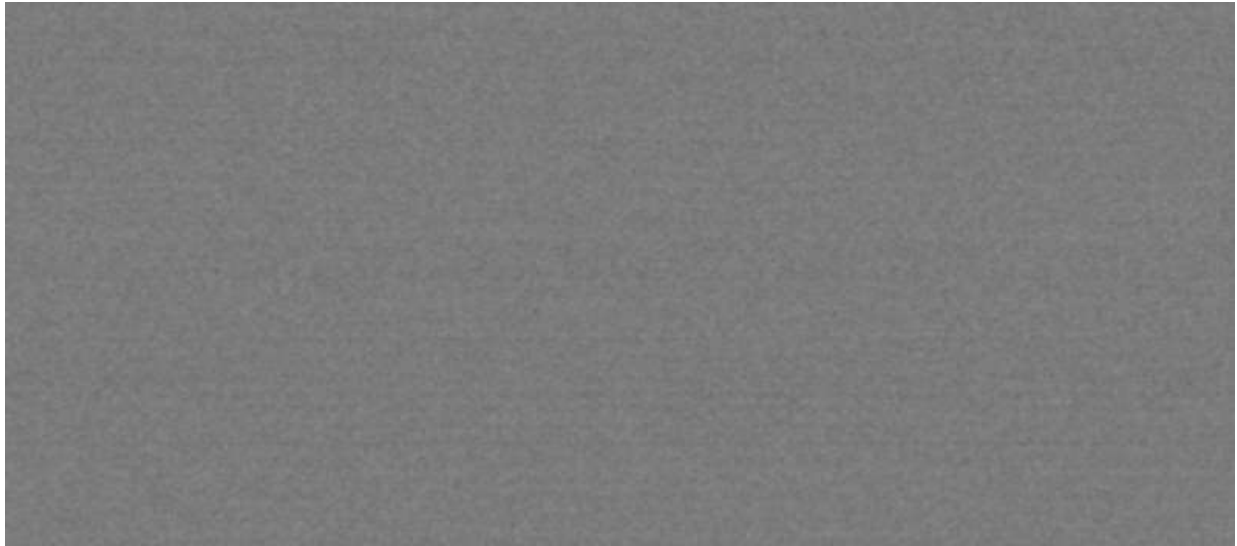
The noise measured in this raw image (made in gain 200) and 1.49 electron. The result after applying the 3x3 median filter:



The RTC noise is largely erased and the noise measured in this image drops to 0.38 electron. This is an important step forward. At the next stage we carry out a median filtering (force 2 in the ISIS repository):



The standard deviation in this last image is 1.79 ADU, the equivalent of an RMS noise of only 0.14 electron. Finally, a 2x2 binning is made for the rest of the operations:



This last step has hardly altered the noise (noise of 0.13 electrons per pixel, close to the scanning noise in fact). The gain in terms of noise is a factor of 10 compared to the original image. This result almost allows you to count the photons one by one (it still lacks a factor 3 to 4 to gain in noise drop to really achieve this feat).

Comparison with CCD imaging is always tricky because the way to perform binning is not at all the same, the same for the nature of noise statistics, pixel size, etc. However, it is reasonable to assume that the equivalent noise of the CCD sensor that equips the ATIK460EX camera after a 2x2 binning, and given the larger size of pixels, is close to 1 electron per pixel. We see that the CMOS sensor operated in the manner described seems superior. This is an important shift in the field of photonic detection and for our spectrographic applications (this result may also be of interest to photon-poor astrophotographers working with narrow spectral bandwidth filters).

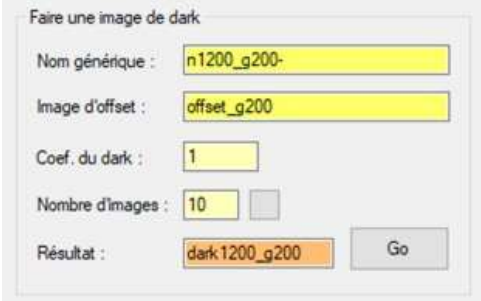
6. Practical use of ISIS software

Version 6 of ISIS adds a tool that makes it easier to implement the CMED algorithm (Instruments/CMOS tab). I will describe its use here, which takes exactly the steps described in the previous section.

But first, we must talk about the conditions of spectrum acquisition and pre-processing, which also have their part in the quality of the final result.

The first point I develop is the question of optimal installation time in very low flow observation. One way to establish a criterion of choice is to look at thermal noise. The method is to calculate the installation time so that thermal noise (equal to the square root of the thermal signal) is close to the reading noise. In this game, given the thermal charge rate of the IMX455 sensor used at -15°C, i.e. only 0.00049 electrons per second (see table at the beginning of this article), this time is around one hour (3600 seconds). This means that the ideal installation time if you have to achieve the spectrum of a very weak object is one hour. And it is probably better to make a unique pose of 3600 seconds than to fragment in 4 poses of 900 seconds, for example. These are quite new considerations in the use of CMOS sensors (note: in planetary imaging with CMOS sensor we accumulate a very large number of images, which and another way to remove THE noise RTS and also to make the selection of images, but here, in very low flow imaging, the very long installation times are very effective, especially thanks to the CMED algorithm, which can effectively eliminate accidents such as cosmic rays).

The use of the CMOS does not remove the importance of making a quality dark signal map with at least the maximum viewing time. For example, here is the calculation of a master image of the thermal signal from a sequence of 10 images posed 1200 seconds taken in darkness (all these images are taken in binning 1x1):



Faire une image de dark

Nom générique : n1200_g200-

Image d'offset : offset_g200


Coef. du dark : 1

Nombre d'images : 10

Résultat : dark1200_g200

Go

The situation of the master image of the offset signal is different with the CMOS sensors. Even with a considerable number of basic images it is very difficult to bring out an image that looks like something other than a constant signal over the entire surface, at least with the IMX455. It's pretty impressive. There is clearly much more to do with a constant electronic bias than with an offset signal that can change depending on where you are on the sensor. In the end, there is no better way than calculating an artificial offset signal using the closest level to that found in characteristic offset images. So here's how I calculate my offset image, so free of noise, and which plays its role perfectly anyway:



Faire une image uniforme

Nom : offset_g200

Constante : 600

Go

In scale spectrography I always realize the flat-fiel (and LED) image by positioning the calibration fiber of 200 microns in front of a 4700 K halogen lamp (museum lighting lamp, SOLUX MR16, 12V 50W). I never use the internal tungsten lamp in the Shelyak calibration box, which is too cold to calibrate spectra in the deep blue with a good signal-to-noise ratio. This is a weakness in equipment that needs to be corrected. So I make a good twenty tungsten images external to the case, thinking of waving the fiber (the "scrambler" evoked at the beginning of the article). The installation time is adjusted to approach the saturation level at the peak (the 16-bit IMX455 detector is particularly appreciated here).

In order to keep a human side to all this, I show you in what condition I make the images of calibrations currently, waiting for the case to be modified so that the procedure can be fully self-labelled: in a closet, in the middle of tomato sauce and small weights, just far from the eShel spectrograph that is cool in its wine cellar. Note the intense halogen lamp 4700 K with the fiber positioned in front on a support. Attention, it is serious, this source of light plays a big part in the success of the observation of the spectrum in the deep blue.



Algorithme CMED

Séquence d'entrée :

Séquence de sortie :

Nombre : ☐

Offset :

Dark :

Filtre médian
☒ 3X3 ☐ 5X5

Binning
☐ 1X1 ☒ 2X2 ☐ 3X3 ☐ 4X4

Filtre gaussien :

Now let's get to the CMED algorithm itself. The screen reproduction on the left shows all the parameters, the tool being accessible from the Instruments/CMOS tab (before version 6 of iSIS it was necessary to go through the command lines CMOS_FULL and CMOS_FULL2, always available).

In the example presented, a sequence of 7 images is treated the comet C2020 F3 NEOWISE (neowise-1, ..., neowise-7). As it should be, these raw images were made in 1x1 binning upon acquisition. The result will be a new sequence of 7 images, which I call here neowise_bin-1, ..., neowise_bin-7. Note, it is very important, that the tool also performs part of the pre-raitment, by making the subtraction of the image master of offset and dark (both obtained in binning 1x1, see above, and I come back later too). A 3x3 median filtering and an internal binning with 2x2 algorithm were chosen for the final image sequence. A median filtering is done with force 2 (if you don't want to filter the image, enter 0). All that's left is to click on Go. If you look at the images neowise_bin-xxx you will see that the size is reduced by a factor of two compared to the original and that the noise is very low.

All that remains is to process the neowise_bin-xxx scale sequence in a (almost) normal way from the ISIS eShel tab:

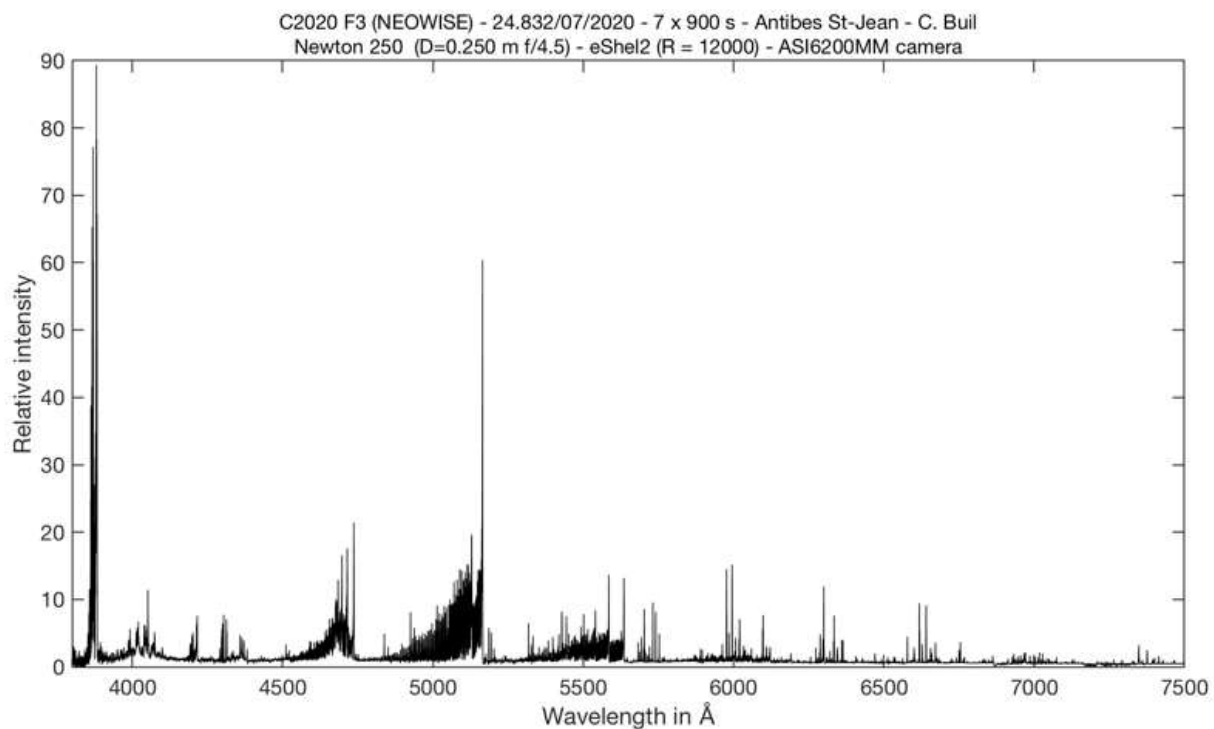
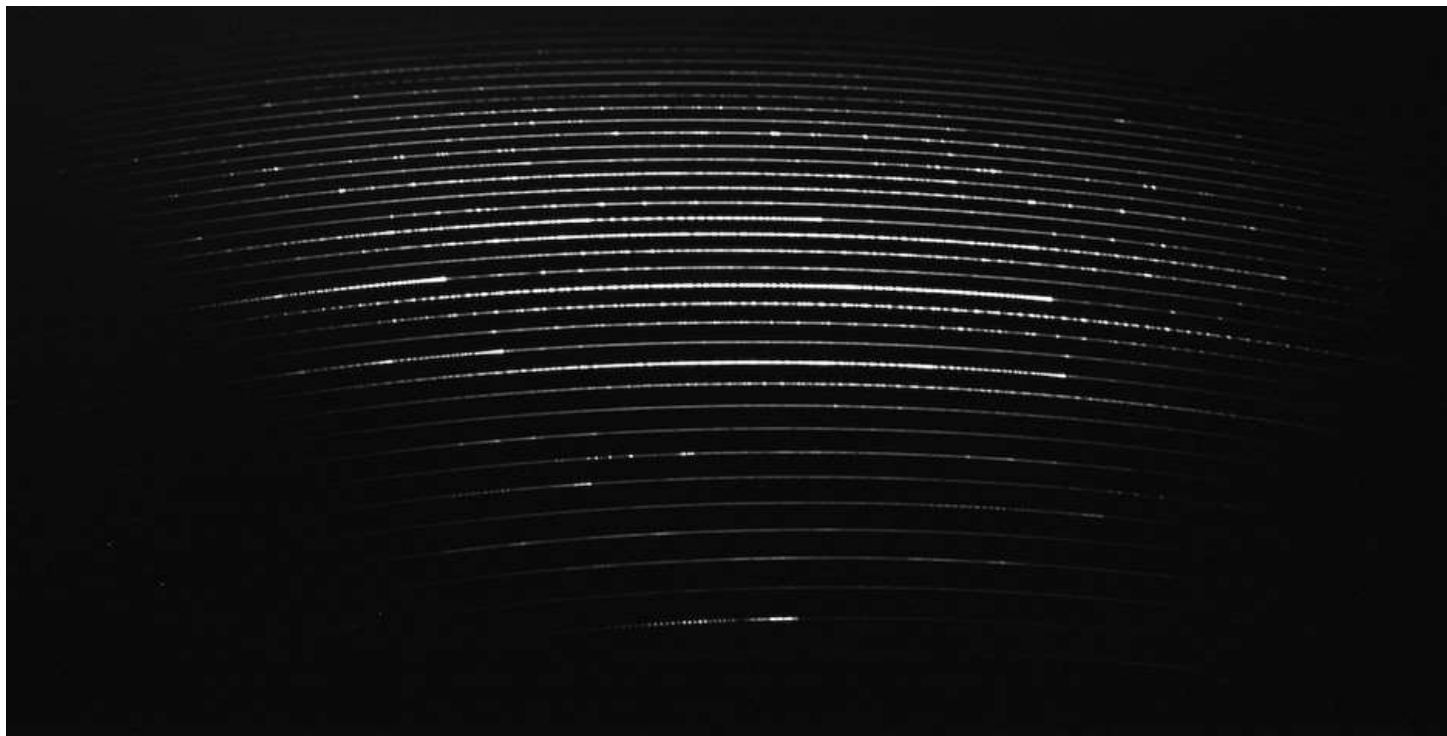
An important difference to note is that the OFFSET, DARK and PRNU fields are left blank, and for good reason, the pre-treatment was carried out with the like CMED. It should not be repeated of course (the PRNU is left out in this version of ISIS because considered not critical in the cellar with the IMX455).

Note that Tung fields. and LEDs are filled with the same image name, that of the tungsten image made in the middle of small weights! Everything else is classic, with the use of optimal binning slightly improved in ISIS V6.

Settings for the spectrograph operating an ASI6200MM can be examined in the following screen copy:

The optimal extraction parameters were slightly modified in version 6 of ISIS (K. Horne algorithm, 1986), with the need now to provide the camera's characteristic reading noise (RON).

The result is a spectacular 2D image of the comet NEOWISE (July 24, 2020), which is the sum of the 7 images neowise_bin-xxx, and corresponding spectral profile:



To be complete, let's talk about the treatment of Tungsten and Thor-Ar images (in the example, the images "tung_neowise" and "thor_neowise" respectively). These are images that are managed in the same way as science objects. This is done in two stages. Here is the example for the tungsten image, knowing that the individual images neowise_tung-xxx are of course made in 1x1 binning:

Algorithme CMED

Séquence d'entrée :

Séquence de sortie :

Nombre : ☐

Offset :

Dark :

Filtre médian

☒ 3X3 ☐ 5X5

Binning

☐ 1X1 ☒ 2X2 ☐ 3X3 ☐ 4X4

Filtre gaussien :

Calculating the pre-processed sequence
neowise_tung_bin-xxx from the raw sequence
neowise_tung-xxx.

Somme d'une séquence d'images

Séquence d'entrée :

Nombre : ☐

Résultat :

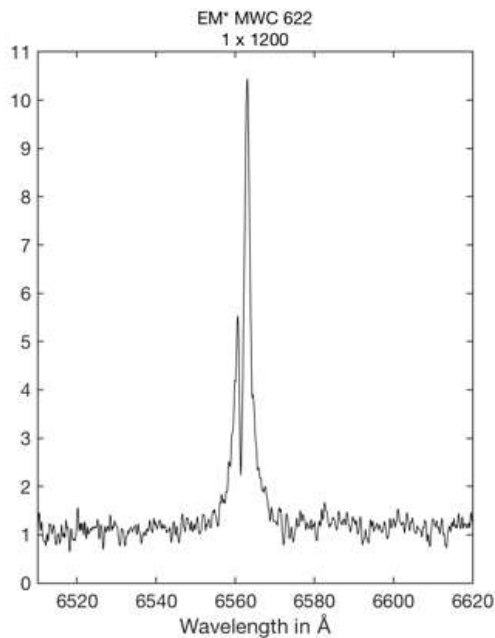
Sum of pre-processed images neowise_tung_bin-xxx to produce
the image tung_neowise high signal-to-noise ratio. Note that you
use a small tool in the CMOS tab to make your life easier.

The same is done strictly in the same way to generate the thor_neowise image from a neowise_thor-xxx sequence. Tip, I usually capture 5 to 7 images of the Thorium-Argon lamp with different poses times, in my case spread between 5 and 30 seconds (some with saturated rays). Making an addition at the end of all these images ultimately gives a high dynamic spectral calibration image that works very well across the spectrum.

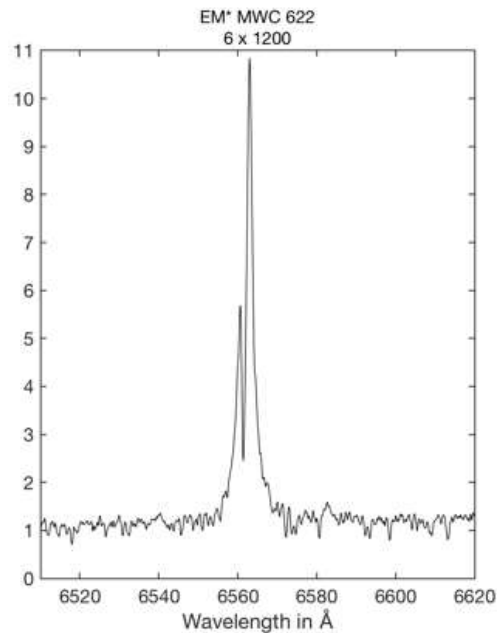
Thanks to the fact that the spectrograph is in the wine cellar, the positioning of the stripes is very stable at night, so I sometimes realize only a sequence of tungsten calibration to Thorium-Argon, which makes the job easier. A wine cellar enhances the wine, it also acts the good spectrographs!

7. Conclusion

In conclusion, here is a spectrum extract centered on the H α ray, that of the star EM MWC 622. It is rich in teaching about the optimization work of eShel that I just presented:

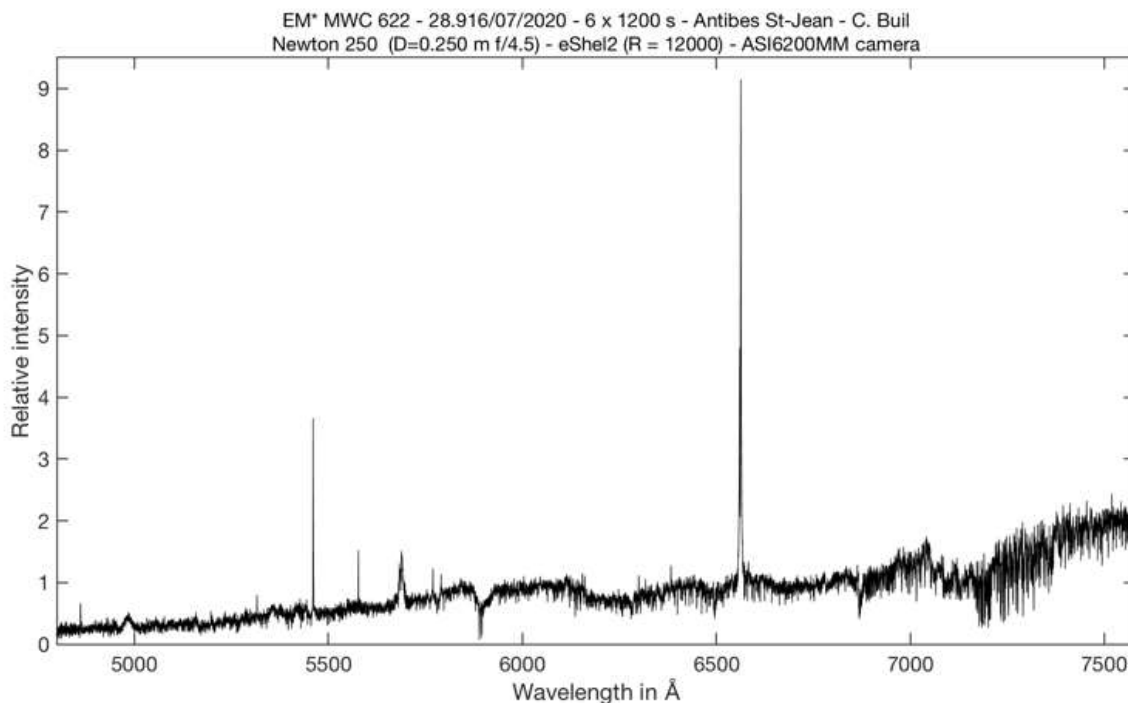


1200s (20 min.) installation time



6 x 1200s installation time (2 hours)

This discrete V-magnitude object is included in the BeSS star base, but had no spectra until then due to its relative brightness weakness. The document shows that one can undertake the observation of stars of this magnitude with eShel and a resolution power $R = 12000$, whereas normally this type of observation is rather reserved for spectrographs with a low spectral resolution. The left-hand spectrum extract corresponds to a laying time of only 20 minutes and a measured signal-to-noise ratio of 14 (RSB - 14), which is enough to properly detail the emission line. The spectrum on the right corresponds to a 2-hour pose under the same conditions (Newton 250 mm f/4.5 telescope, ASI6200MM camera). The signal-to-noise ratio is now 30 (RSB - 30), which allows us to study the continuum, riddled with fine rays. In two hours of installation it is therefore possible to reach V 13 with an RSB of 15 in the continuum with a telescope all in size, 250 mm in diameter. The power of eShel is also expressed when looking at a large spectral domain: the star EM-MWC 622 is far too red to be a Be-type object:



Several technical initiatives to improve the eShel spectrograph were presented. . The optics were modified to turn off the observation area to blue and the latest CMOS camera model could be tested on it. The whole thing forms a very coherent whole. The performance of the CMED algorithm and its implementation in the ISIS software have been shown and quantified. All this provides a second youth to this instrument.

[Back](#)